

The geometry of bipartite qutrits including bound entanglement

B. Baumgartner, B.C. Hiesmayr*, H. Narnhofer

Faculty of Physics, University of Vienna, Boltzmannngasse 5, 1090 Vienna, Austria

We investigate the state space of bipartite qutrits. We construct an analog to the “magic” tetrahedron for bipartite qubits—a magic simplex \mathcal{W} . It is formed by all convex combination of nine Bell states which are constructed using Weyl operators. Due to the high symmetry it is enough to consider certain typical slices through \mathcal{W} . Via optimal entanglement witnesses we find regions of bound entangled states.

I. INTRODUCTION

Quantum entanglement is without doubt one of the most remarkable features of quantum mechanics. It is the source of applications like quantum cryptography, teleportation, dense coding or a possible quantum computer. Up to now one does not yet have a good computable way to distinguish entangled states from separable ones for higher dimension or more particles and not much is known about the structure of the set of separable states. In this letter we explore a subset of bipartite qutrit states for which we find the geometrical structure, surprisingly including a whole region of bound entangled states.

To explore the geometrical structure, as is the main topic of many works (e.g. Ref. [2, 3, 4, 5, 6, 7, 8]), is of great help in understanding the quantum features, develop quantum measures and algorithms and hence to find future applications.

Since the seminal letter on distillation [1], it was a common expectation that all entangled bipartite states are distillable, but already for bipartite qutrits one finds states which are positive under partial transpose PT , i.e. have only positive eigenvalues, called PPT states, but cannot be distilled [9], i.e. by no local operation and classical communication (LOCC) Alice and Bob can purify or distill this bipartite mixed state into a maximally entangled one. These states are called *bound* entangled. Though a lot of examples are found, e.g. Refs. [10, 11, 12, 13, 14], and even for thermal states (e.g. Ref. [15] and references therein), general recipes to construct such kind of states are lacking. The reason for the existence of these kind of states is also unknown and still mysterious [16].

We start by considering a subset of bipartite qubits for which the state space can be visualized via the “magic” tetrahedron [17, 18]. We find for bipartite qutrits a subset where an analogous simplex can be drawn. We analyze the set of separable states within and point out the similarities to bipartite qubits, and discuss the differences, e.g. the polytope structure and bound entanglement.

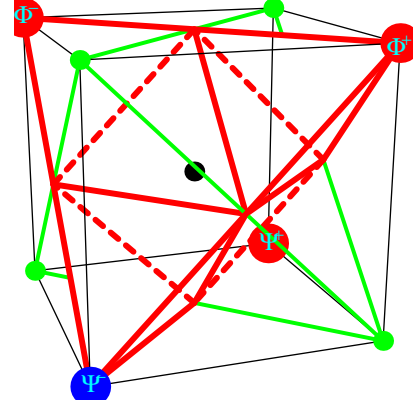


FIG. 1: (Color online) For two qubits four orthogonal Bell states, ψ^\pm, ϕ^\pm can be used to decompose every locally maximally mixed state and a geometric picture can be drawn. The positivity condition forms a tetrahedron (red) with the four Bell states at the corners of the cube and the totally mixed state, the trace state, in the origin (black dot in the middle). Via reflection $\vec{c} \rightarrow -\vec{c}$ one obtains another tetrahedron (green) with reflected Bell states located in the remaining corners of the cube. The intersection of both tetrahedra gives an octahedron where all points inside and at the surface represent separable states.

II. BIPARTITE QUBITS

A single qubit state ω lives in a two dimensional Hilbert space, i.e. $\mathcal{H} \equiv \mathbb{C}^2$, and any state can be decomposed into the well known Pauli matrices

$$\omega = \frac{1}{2} (\mathbb{1}_2 + n_i \sigma^i)$$

with the Bloch vector components $\vec{n} \in \mathbb{R}^3$ and $\sum_{i=1}^3 n_i^2 = |\vec{n}|^2 \leq 1$. For $|\vec{n}|^2 < 1$ the state is mixed (corresponding to $\text{Tr} \omega^2 < 1$) whereas for $|\vec{n}|^2 = 1$ the state is pure ($\text{Tr} \omega^2 = 1$).

The density matrix of 2-qubits ρ on $\mathbb{C}^2 \otimes \mathbb{C}^2$ is usually obtained by calculating its elements in the standard product basis, i.e. $|00\rangle, |01\rangle, |10\rangle, |11\rangle$. Alternatively, we can write any 2-qubit density matrix in a basis of 4×4 matrices, the tensor products of the identity matrix $\mathbb{1}_2$ and the Pauli matrices σ^i ,

$$\rho = \frac{1}{4} (\mathbb{1}_2 \otimes \mathbb{1}_2 + a_i \sigma^i \otimes \mathbb{1}_2 + b_i \mathbb{1}_2 \otimes \sigma^i + c_{ij} \sigma^i \otimes \sigma^j)$$

*Beatrix.Hiesmayr@univie.ac.at

with $a_i, b_i, c_{ij} \in \mathbb{R}$. The parameters a_i, b_i are called *local* parameters as they determine the statistics of the reduced matrices, i.e. of Alice's or Bob's system. In order to obtain a geometrical picture as in Ref. [17, 18] we consider in the following only states where the local parameters are zero ($\vec{a} = \vec{b} = \vec{0}$), i.e., the set of all locally maximally mixed states, $Tr_A(\rho) = Tr_B(\rho) = \frac{1}{2}\mathbb{1}_2$.

A state is called separable if and only if it can be written in the form $\sum_i p_i \rho_i^A \otimes \rho_i^B$ with $p_i \geq 0, \sum p_i = 1$, otherwise it is entangled. As the property of separability does not change under local unitary transformation and classical communication (LOCC) the states under consideration can be written in the form [18]

$$\rho = \frac{1}{4} (\mathbb{1}_2 \otimes \mathbb{1}_2 + c_i \sigma^i \otimes \sigma^i),$$

where the c_i are three real parameters and can be considered as a vector \vec{c} in Euclidean space. In Fig. 1 we show a 3-dimensional picture, where each point \vec{c} corresponds to a locally maximally mixed state ρ . The origin $\vec{c} = \vec{0}$ corresponds to the totally mixed state, i.e. $\frac{1}{4}\mathbb{1}_2 \otimes \mathbb{1}_2$. The only pure states in the picture are given by $|\vec{c}| = 3$ and represent the four maximally entangled Bell states $|\psi^\pm\rangle = \frac{1}{\sqrt{2}}\{|01\rangle \pm |10\rangle\}, |\phi^\pm\rangle = \frac{1}{\sqrt{2}}\{|00\rangle \pm |11\rangle\}$.

It is well known that density matrices which have at least one negative eigenvalue after partial transpose (PT), i.e. $\mathcal{T} \otimes \mathbb{1}$ (\mathcal{T} ...transposition), are entangled. The inversion of the argument is only true for systems with $2 \otimes 2$ and $2 \otimes 3$ degrees of freedom. PT corresponds to a reflection, i.e. $c_2 \rightarrow -c_2$ with all other components unchanged. Thus all points inside and at the surface of the octahedron represent all separable states in the set.

III. BIPARTITE QUTRITS

The description of single qutrits can be made very similar to the one for qubits, i.e. any qutrit state $\omega \in \mathcal{H}^3 \equiv \mathbb{C}^3$ can then be expressed by

$$\omega = \frac{1}{3} (\mathbb{1}_3 + \sqrt{3} n_i \lambda^i), \quad n_i \in \mathbb{R}, \quad \sum_{i=1}^8 n_i^2 = |\vec{n}|^2 \leq 1,$$

where λ^i ($i = 1, \dots, 8$) are the eight Gell-Mann matrices, generalized Pauli matrices, with properties $\text{Tr} \lambda^i = 0$, $\text{Tr} \lambda^i \lambda^j = 2 \delta^{ij}$. However, whereas for qubits all Bloch vector's form a unit sphere and describe density matrices, not all 8-dimensional Bloch vectors for qutrits describe necessarily a density matrix. For example $n_8 = 1$ and all other components equal zero describes a matrix which is not positive definite. The full analogy between single qubits and qutrits already fails.

For bipartite qutrits we could now try to follow an analogous way as for qubits, i.e., consider only density matrices where the local parameters are set to zero. However, not all locally maximally mixed states can be decomposed into maximally entangled states, the Bell

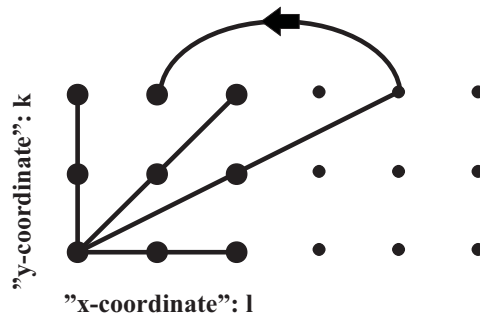


FIG. 2: Here we plotted the points $P_{k,l}$ of the discrete classical phase space. l denotes the values of the position coordinate and runs from 0 to 2 and k “quantizes” the momentum and runs also from 0 to 2. From one fixed point, e.g. $P_{0,0}$, all possible lines are drawn. Thus the phase space carries 4 bundles where each bundle consists of 3 parallel lines. In Ref. [21] it is shown that transformations inside the simplex \mathcal{W} are equivalent to transformations in this phase space and that the lines are all equivalent in the sense that each line may be transformed into any other one. This enables us to study the geometry of separability and PPT in \mathcal{W} by e.g. just considering 3 Bell states on a line.

states for qutrits. Thus we have to reduce the set of all locally maximally mixed states further and we do that with the help of an alternative way to generalize the Pauli matrices, i.e. by unitary matrices which are not Hermitian, see e.g. Ref. [19, 20].

IV. THE CONSTRUCTION OF THE MAGICAL SIMPLEX \mathcal{W}

We start with a maximally entangled pure state, this is a Bell type state, in a chosen basis $\{0, 1, 2\}$

$$\Omega_{00} = \frac{1}{\sqrt{3}} \sum_{s=0}^2 |s\rangle \otimes |s\rangle.$$

On the first subspace, the system of Alice, we act with the Weyl operators, defined by $W_{k,l}|s\rangle = w^{k(s-l)}|s-l\rangle$ with $w = e^{2\pi i/3}$, while Bob's subsystem is always left inert. The indexes k and l run from 0 to 2. The other eight Bell states are constructed by acting with the Weyl operators onto the chosen Bell state

$$\Omega_{k,l} = W_{k,l} \otimes \mathbb{1}_3 \Omega_{0,0}.$$

With that we can construct nine Bell projectors $P_{k,l} = |\Omega_{k,l}\rangle\langle\Omega_{k,l}|$. The mixtures of these pure states form our object of interest, the **magic simplex** \mathcal{W} :

$$\mathcal{W} = \left\{ \sum c_{kl} P_{k,l} \mid c_{kl} \geq 0, \quad \sum c_{kl} = 1 \right\}.$$

Our aim is to discuss the geometry of this 8-dimensional simplex in the context of separability and entanglement.

We focus mainly on entanglement detected by PT and give examples for a whole region of bound entangled states, i.e. states which are PPT but not separable, for a certain class of states.

Clearly, the same construction can be used for qubits, i.e. choose any Bell state, e.g. $\Omega_{0,0} = |\phi^+\rangle$, act on one subspace with the Weyl operators $W_{k,l}$ where $w = e^{2\pi i/2} = -1$ and k, l runs from 0 to 1 (equivalent to the Pauli matrices). One obtains all four Bell states; this also generalizes for any bipartite qudit system.

Let us remark that for qutrits not all locally maximally mixed states can be diagonalized by Bell type states and even if so, they may not be embedded into a version of \mathcal{W} . Moreover, there exist nine mutually orthogonal Bell type states which do not form an equivalent to \mathcal{W} . Examples and proofs can be found in Ref. [21, 22] as well as how \mathcal{W} is embedded in the whole state space.

Of course it is difficult to draw a picture of this 8-dimensional simplex, however, it can be considerably simplified because of the high symmetry inside \mathcal{W} . This means that certain mixtures of Bell states, $P_{k,l}$, form equivalence classes: The indexes k and l of the Bell states $P_{k,l}$ can be interpreted as the “quantized” momentum and position coordinate, respectively. In Fig. 2 we have drawn such a phase space interpretation. It turns out that the symmetry of \mathcal{W} —appearing as reflection, rotation and shear in the phase space—is such that all states on a line, as indicated in Fig. 2, have the same geometry concerning separability and entanglement. This means states which are mixtures of the unity and three Bell states on a line can be handled on the same footing, which is done in the next section. Another geometrical picture is obtained if one chooses any two Bell states, which clearly define a certain line, and any other Bell state which does not belong to this line, this is studied at the end.

This describes the full geometry of those states which can be decomposed into the unity and three Bell states and is discussed in the following. Of course to get the full geometry one has to consider also mixtures of more than three Bell states.

A. The geometry on a line

As a first example let us consider the states

$$\rho = \frac{1 - \alpha - \beta}{9} \mathbb{1}_3 \otimes \mathbb{1}_3 + \alpha P_{0,0} + \frac{\beta}{2} (P_{1,0} + P_{2,0}). \quad (1)$$

The geometry is given in Fig. 3 (b). The positivity condition ($\rho \geq 0$) is satisfied for all points $\{\beta, \alpha\}$ inside the (green) triangle (only 3 different eigenvalues). All states positive under PT , $(\mathcal{T} \otimes \mathbb{1}_3)\rho \geq 0$, have to be inside the dotted (blue) triangle (only 3 different eigenvalues). The intersection of both triangles corresponds to either separable or bound entangled states. To find out whether the dotted area also includes bound entangled states, one has to construct optimal tangential wit-

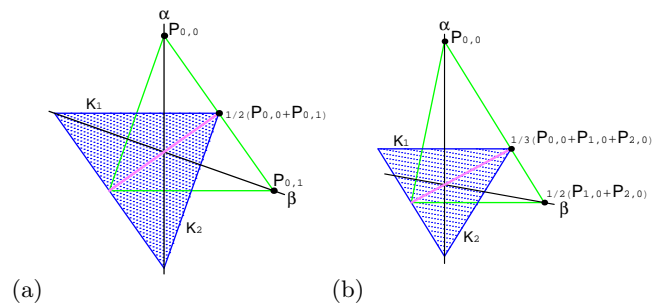


FIG. 3: The left figure visualizes the geometry corresponding to the bipartite qubit states $\rho = \frac{1-\alpha-\beta}{4} \mathbb{1}_4 + \alpha P_{0,0} + \beta P_{0,1}$ and the right figure the geometry corresponding to the bipartite qutrit states $\rho = \frac{1-\alpha-\beta}{9} \mathbb{1}_9 + \alpha P_{0,0} + \frac{\beta}{2} (P_{0,1} + P_{0,2})$. The green triangle presents positivity and the dotted blue triangle all matrices positive under partial transpose (PPT). The axes are chosen in such a way that the symmetry of \mathcal{W} becomes a geometrical symmetry. In both cases it turns out that the intersection of positivity and PPT equals separability, thus the two (blue) border lines of PPT crossing the axes, K_1, K_2 , are optimal tangential witnesses for the states represented. While for qubits this includes the whole symmetry on a line, for qutrits we have also other symmetries, see Fig. 4.

nesses. An entanglement witness for a given state ρ is a criterion to decide whether ρ is inside the set of all separable states, i.e. \mathcal{S} (see also Refs. [23, 24, 25]). The set of tangential witnesses K for a state ρ is defined by $\{K = K^\dagger \neq 0 | \forall \sigma \in \mathcal{S} : Tr(K\sigma) \geq 0, Tr(K\rho) = 0\}$.

In the qubit case the planes of the octahedron in Fig. 1 or the lines in Fig. 3 (a) represent such tangential entanglement witnesses, K_1, K_2 , which are optimal for discriminating between separable and entangled states. In Ref. [21] it is proven that a witness for states on a line mixed with unity must have the form

$$K = \lambda \frac{1}{3} \mathbb{1}_3 \otimes \mathbb{1}_3 + \sum_k \kappa_k P_{k,0}.$$

Furthermore, K is directly related to the matrices

$$M_\Phi = \lambda \mathbb{1}_3 + \sum_k \kappa_k W_{k,0} |\Phi\rangle \langle \Phi| W_{k,0}^\dagger$$

with Φ being any normalized state vector in \mathbb{C}^3 . If M_Φ is non-negative $\forall \Phi$, K is a witness and moreover if $\det M_\Phi = 0$, then K is a tangential witness.

For the states (1) it turns out that K_1, K_2 —the limiting lines of PT —are optimal tangential witnesses, i.e. $\det M_\Phi = 0$ for certain Φ 's. This means the dotted area inside positivity represents separable states, i.e. $PPT \equiv$ separable, see Fig. 3 (b).

Generally, any state on a line and unity is given by

$$\rho = \frac{1 - \alpha - \beta - \gamma}{9} \mathbb{1}_3 \otimes \mathbb{1}_3 + \alpha P_{0,0} + \beta P_{1,0} + \gamma P_{2,0}. \quad (2)$$

and the geometry is drawn in Fig. 4. The positivity condition on the three eigenvalues forms again a triangle, the

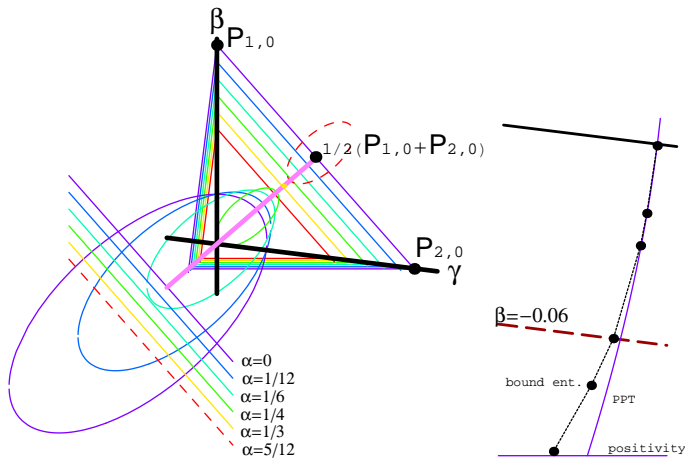


FIG. 4: The left figure visualizes the slices through the state space $\rho = \frac{1-\alpha-\beta-\gamma}{9} \mathbb{1}_3 \otimes \mathbb{1}_3 + \alpha P_{0,0} + \beta P_{1,0} + \gamma P_{2,0}$, where the biggest triangle (\equiv positivity) and the biggest ellipse/line (\equiv PPT) correspond to $\alpha = 0$ (purple), the next biggest objects to $\alpha = \frac{1}{12}$ (blue) and so on until $\alpha = \frac{5}{12}$ (dashed, red). For $\alpha < \frac{1}{6}$ the PPT region is an ellipse cut by a line and for $\frac{1}{6} \leq \alpha < \frac{5}{12}$ it is solely an ellipse. In the last case ($\alpha = \frac{5}{12}$) the PPT area does not intersect the positivity area (smallest, red triangle), that means all states are entangled, in agreement to Fig 3 (b). Contrary to the slice in Fig 3 (b) not all PPT states are separable. In the figure to the right hand side an enlargement for negative β and $\alpha = 0$ is shown. The dots are the density matrices for which the tangential witness is optimized. That means all states between the iterated curve and the PPT ellipse correspond to bound entangled states.

condition on PT , however, forms a more complicated object (an ellipse and a line). As one mixes more and more $P_{0,0}$ to the state, the region of positivity and PPT decreases, until for $\alpha > \frac{1}{3}$ both regions do not intersect anymore, i.e. only entangled states are found. For $\alpha = \frac{1}{3}$ a single point, the line state, is separable. **Again we have to ask whether the states positive under PT are all separable?**

In Ref. [21] the case $\alpha = 0$ is discussed and indeed it turns out that there is a small region of bound entangled states if either β or γ is negative (see enlarged region, right hand side of Fig. 4). The difference between the PPT boundary and separability is rather small, at most of the order 10^{-2} . **The question arises whether the bound entangled region increases or decreases when $P_{0,0}$ is more and more mixed to the state.**

Here we can distinguish two cases, i.e. $P_{0,0}$ is mixed with positive or negative α . If we choose for instance $\beta = -0.06$ (see also Fig. 5) we find that for $\alpha \geq 0$ the region decreases, i.e. already for $\alpha = 1/12$ we find no better witness than given by PPT up to numerical precision of 10^{-6} (using standard optimization methods). For $\alpha \leq 0$ the region decreases until for $\beta = \gamma = -0.06$ no bound entangled state is found and then increases again. Clearly in the case $\beta = \gamma = -0.06$ we have the case represented

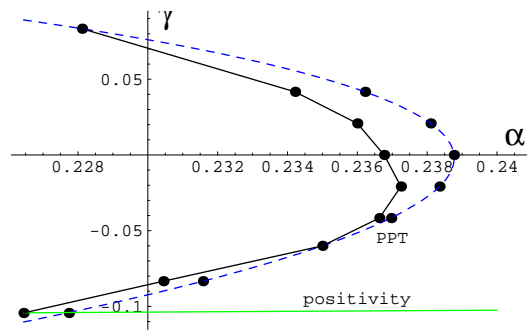


FIG. 5: The figure visualizes the slices through the state space $\rho = \frac{1-\alpha-\beta-\gamma}{9} \mathbb{1}_3 \otimes \mathbb{1}_3 + \alpha P_{0,0} + \beta P_{1,0} + \gamma P_{2,0}$ with $\beta = -0.06$. On the horizontal axis α and on the vertical axis γ is plotted. The (green) line represents the positivity border and the dashed (blue) curve the PPT border. The points are derived by optimizing the witness and therefore represent the separability border. Between the two curves one has the bound entangled states. Note that clearly for $\beta = \gamma = -0.06$ the state is not bound entangled for any α , see Fig. 3 (b).

by Fig. 3 (b) where no bound entangled states can be found.

The “generalized” concurrence for qutrits [26] turns out to give the same result for $\gamma = 0$ for certain numerical quasi pure approximations [27]. Also for $\gamma = \pm \frac{1}{12}$ the results coincide.

Summarizing, the geometry of mixtures of three Bell states on a line and the unity is such that separable and bound entangled states form sections through the simplex, where the bound entangled states form only a small region, see also Fig. 3 (b), Fig. 4 and Fig. 5.

B. The geometry beyond lines

The second possibility of a mixture of 3 Bell states is to choose two Bell states which always define a line and choose any other Bell state which is not the one completing the line and mix it with the unity, e.g.

$$\rho = \frac{1-\alpha-\beta-\gamma}{9} \mathbb{1}_3 \otimes \mathbb{1}_3 + \alpha P_{10} + \beta P_{20} + \gamma P_{11}. \quad (3)$$

Clearly, the positivity condition gives the same three different eigenvalues as in the cases before. However, if one chooses $\beta, \gamma \rightarrow \frac{\beta}{2}$, the boundary of PPT consists no longer of simple lines, see Fig. 6 (a). If one considers slices spanned up by the unity and two Bell states, Fig. 6 (b), we obtain no longer a cone but a more complex object.

In principle any optimal witness can be calculated with the procedure as given in Ref. [21], more parameters, however, are involved and consequently it is hard to minimize $\det M_{\Phi}$. For that another numerical strategy is necessary and will be done in a future work. Calculation with the ‘generalized’ concurrence for qutrits [26] for certain numerical quasi pure approximations [27] have shown that there are also bound entangled regions in this case.

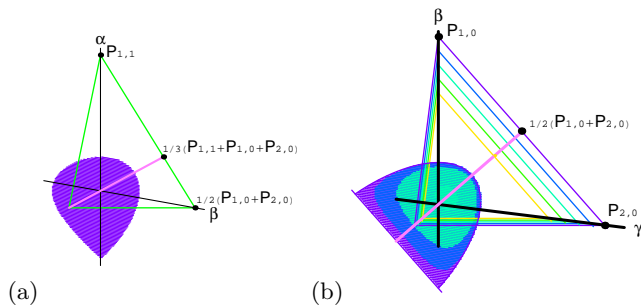


FIG. 6: Both figures visualize the state space $\rho = \frac{1-\alpha-\beta-\gamma}{9} \mathbb{1}_9 + \alpha P_{10} + \beta P_{20} + \gamma P_{11}$, where in (a) $\beta, \gamma \rightarrow \frac{\beta}{2}$ and in (b) slices with $\alpha = 0, \frac{1}{12}, \frac{1}{6}, \frac{1}{4}, \frac{1}{3}$ are shown (color coding as in Fig. 4). Compared to the line case, Fig. 3 (b) and Fig. 4, the *PPT* region is more complicated, i.e. is not simply an ellipse. The *PPT* region shrinks with increasing α and already for $\alpha = \frac{1}{3}$ (smallest (yellow) triangle) no separable state is found.

V. SUMMARY

We discuss the state space of locally maximally mixed bipartite qubits, i.e. such states where the trace over one party gives the normalized unity. A three dimensional picture of the geometry of separability and entanglement can be drawn, Fig. 1. We generalize for bipartite qutrits, where a certain smaller state space, a subspace of all locally maximally mixed density matrices, is considered. We obtain it by acting with the Weyl operators, generalized Pauli matrices, onto a chosen maximally entangled state, a Bell state. In this way one can construct nine Bell states and its convex combination forms our object of interest, the magic simplex \mathcal{W} .

It has nine Bell states in the corners and given the high symmetry of this state space, one finds a phase-space structure, see Fig. 2, implying that certain Bell states form equivalency classes.

We investigate the geometry of \mathcal{W} , in particular the geometry of three such Bell states forming a line mixed with the unity, see Fig. 3 and Fig. 4. We find that the separable states do not form a simple polytope as in the qubit case and despite the fact that only a subset of all locally maximally mixed states is considered we find even a whole region of bound entangled states. They are obtained by optimizing bound entanglement witnesses. The high symmetry on a line reduces the class of witnesses remarkably and consequently optimization is numerically obtainable. Furthermore, we find that the region of bound entangled states decreases/increases if the third state of the line is mixed to it.

Last but not least we investigate the state space of two Bell states, the unity and another Bell state not on the line formed by the previous ones. The region representing the states positive under partial transpose (*PPT*) show a even more complicated geometry, see Fig. 6.

Concluding, while for bipartite qubits the geometry of separability and entanglement is exhausted by considering a line—the mixture of the unity and any two Bell states—for bipartite qutrits the geometry is more complicated and includes new phenomena which may find interesting applications in future.

Acknowledgements: Many thanks to Simeon Sauer, Fernando de Melo, Joonwoo Bae, Florian Mintert and Andreas Buchleitner for providing us with their numerical results of the “generalized” concurrence.

-
- [1] C.H. Bennett, G. Brassard, S. Popescu, B. Schumacher, J. Smolin, and W.K. Wootters, Phys. Rev. Lett. **78**, 2031 (1996).
 - [2] H. Narnhofer, J. Phys. A **39**, 7051 – 64.
 - [3] K. G. H. Vollbrecht, R. F. Werner, Phys. Rev. A **64**, 062307 (2001).
 - [4] J.M. Leinaas, J. Myrheim, E. Ovrum, Phys. Rev. A **74**, 012313 (2006).
 - [5] O. Pittenger, M.H. Rubin, Lin. Alg. Appl. **390**, 255 (2004).
 - [6] W.K. Wootters: *Quantum measurements and finite geometry*; arXiv:quant-ph/0406032.
 - [7] I. Bengtsson: *MUBs, polytopes and finite geometries*; arXiv:quant-ph/0406174.
 - [8] K.G.H. Vollbrecht, R.F. Werner: J. Math Phys. **41**, 6772 (2000).
 - [9] M. Horodecki, M. Horodecki, and R. Horodecki, Phys. Rev. Lett. **80**, 5239 (1998).
 - [10] R. Augusiak, J. Stasinska and P. Horodecki, “*Beyond the standard entropic inequalities: stronger scalar separability criteria and their applications*”, arXiv: 0707.431.
 - [11] H.-P. Breuer, Phys. Rev. Lett. **97**, 080501 (2006).
 - [12] L. Derkacz and L. Jakobczyk. “*Entanglement of a class of mixed two-qutrit states*”, arXiv: 0707.1575.
 - [13] M. Nathanson and M.B. Ruskai, Mathematical Systems Theory **40**, 8171 (2007).
 - [14] M.R.P. Planat, H. Rosu, S. Perrine and M. Saniga, Foundations of Physics **36**, 1662 (2006).
 - [15] D. Cavalcanti, A. Ferraro, A. Garcia-Saez and A. Acin, *Thermal bound entanglement and area laws*, arXiv: 0705.3762.
 - [16] R. Horodecki, P. Horodecki, M. Horodecki and K. Horodecki, “*Quantum entanglement*”, arXiv: 0702.225.
 - [17] R. Horodecki and M. Horodecki, Phys. Rev. A **54**, 1838 (1996).
 - [18] R.A. Bertlmann, H. Narnhofer, and W. Thirring, Phys. Rev. A **66**, 032319 (2002).
 - [19] H. Weyl: *Gruppentheorie und Quantenmechanik*, zweite Auflage, (S. Hirzel, Leipzig, 1931).
 - [20] D. Gottesman, A. Kitaev, and J. Preskill, Phys. Rev. A **64**, 012310 (2001).
 - [21] B. Baumgartner, B.C. Hiesmayr, and H. Narnhofer, Phys. Rev. A **74**, 032327 (2006).
 - [22] B. Baumgartner, B.C. Hiesmayr, and H. Narnhofer, J.

- Phys. A **40**, 7919 (2007).
- [23] R.A. Bertlmann, K. Durstberger, B.C. Hiesmayr and P. Krammer, Phys. Rev. A **72**, 052331 (2005).
- [24] R.A. Bertlmann and Ph. Krammer, “*Bloch vectors for qudits and geometry of entanglement*”, arXiv: 0706.1743.
- [25] R.A. Bertlmann and Ph. Krammer, “*Geometric entanglement witnesses and bound entanglement*”, arXiv: 0710.1184.
- [26] F. Minert, M. Kus and A. Buchleitner, Phys. Rev. Lett. **92**, 167902 (2004).
- [27] S. Sauer, F. de Melo, J. Bae, F. Mintert and A. Buchleitner, *private communication*.